ELSEVIER

Journal of Chromatography A, 806 (1998) 31–45

JOURNAL OF CHROMATOGRAPHY A

Preparative purification of supercoiled plasmid DNA using anion-exchange chromatography

Duarte Miguel F. Prazeres[a,b,*], Thomas Schluep[b], Charles Cooney[b]

[a]*Centro de Engenharia Biológica e Química, Instituto Superior Técnico, Avenida Rovisco Pais, 1000 Lisbon, Portugal*

[b]*Chemical Engineering Department, Massachusetts Institute of Technology, 77 Massachusetts Avenue, Cambridge, MA 02139, USA*

Abstract

Large scale manufacturing of gene vectors such as plasmid DNA is an important issue in gene therapy. Anion-exchange chromatography is fundamental in the downstream processing of plasmids both as a process and analytical technique. This work reports the use of Q-Sepharose columns (1, 10 and 40 ml) for the preparative purification of plasmid pUC18. NaCl gradient elution enabled the isolation of supercoiled plasmid from low-M_r RNA, cDNA and plasmid variants. A compact covalently closed, supercoiled form of denatured plasmid carrying large stretches of single-stranded DNA was identified as one of the major contaminants. Anion-exchange HPLC on a Poros QE 20 column was used to quantify plasmid yield. Supercoiled plasmid was recovered in a single fraction with a 62±8% yield. Loadings higher than 40 μg/ml gel could be used but at the expense of a loss of resolution between open circular and supercoiled forms. Plasmid quality was evaluated by gel electrophoresis, restriction analysis, transformation experiments and protein assays. © 1998 Elsevier Science B.V.

Keywords: Preparative chromatography; Plasmid DNA; Gene therapy

1. Introduction

Gene therapy is a promising process for the prevention, treatment, cure and diagnosis of diseases like cancer, acquired immune deficiency syndrome (AIDS) or cystic fibrosis. One of the methods used to administer therapeutic genes is the direct injection of ''naked'' or lipid-coated plasmid DNA into the target tissues [1]. This mode of treatment requires considerable amounts of pharmaceutical-grade plasmid. A typical dose size, for instance as used in the case of patients with melanoma is 0.3 μg, but full treatments could require milligram quantities of plasmid DNA [2]. The development of large scale production and purification processes, capable of reproducibly meeting the demanding standards of regulatory agencies [3] in terms of purity, potency, safety and efficacy is a challenge for the biochemical engineer [4,5].

Plasmids for gene therapy are usually produced in *Escherichia coli* host by fermentation. The majority of the plasmid molecules isolated from prokaryotes such as *E. coli* are negatively supercoiled (sc) with a long, thin and branched structure which is better adapted to an active role in cell physiology [6,7]. A fraction of the population of plasmid molecules also can exist in a relaxed or open circular (oc) form, with no coiling of the double helix. Other variants such as linear, denatured or dimeric also can be present in the culture media. The challenge in downstream processing is essentially aimed at eliminating cellular components of the host like bacterial proteins, lipids, lipopolysaccharides and nucleic acids. Chromosomal

*Corresponding author. Corresponding address: Centro de Engenharia Biológica e Química, Instituto Superior Técnico, Avenida Rovisco Pais, 1000 Lisbon, Portugal.

0021-9673/98/$19.00
PII S0021-9673(97)01254-5

DNA (cDNA) fragments obtained after cell lysis, high-molecular-mass RNA (ribosomal and messenger RNA) and plasmid variants, which may be ineffective in transferring gene expression [8], are particularly difficult to separate from supercoiled plasmids due to the similarities in the physical and chemical structure.

Chromatography is central to the large-scale purification of plasmids, both as a process step and as an analytical tool used for monitoring process development and quality control. Different types of chromatography such as gel filtration [5,9], ion-exchange [10–15], reversed-phase [16] and affinity [17] have been used for the separation of plasmid DNA. Plasmid purification by anion-exchange chromatography takes advantage of the interaction between the negatively charged phosphate groups in the DNA backbone and the positively charged ligands on the matrix surface. After binding, a salt gradient is used to displace the different nucleic acids which in principle should elute in order of increasing overall net charge, which in turn is a function of chain length [18]. The shape and size of the molecules also may play an important role, particularly in the separation of plasmid variants. In fact, in some anion exchangers, the more compact supercoiled forms, which have a higher charge density, elute later than the open circular forms which have a lower, overall, charge density [10,12–14]. Base sequence and composition also are known to affect the elution pattern of nucleic acids in anion exchangers [19]. Because plasmids are very large molecules ($M_r > 1 \cdot 10^6$), their binding to the majority of the existent commercial anion exchangers is likely to occur only at the surface. This constitutes an important capacity limitation especially in preparative applications. Nevertheless, the question of whether plasmids can penetrate even some of the large pore particles such as perfusion materials has not been satisfactory answered.

Several authors have reported on the analytical and/or preparative anion-exchange chromatography of plasmids using weak anion-exchange ligands such as DEAE coupled to silica [12] or polymer-based matrices [13], and strong ligands such as quaternary amines coupled to polymeric matrices [10,14]. The use of a composite media made of a porous ceramic skeleton whose pores are filled with a polyacrylamide gel, with both Q and DEAE groups has also been described recently [15].

Despite these reports, process questions related to the purification of supercoiled plasmid, such as yields, reproducibility, loadings, scale-up and DNA quality have not been fully addressed so far. This paper describes the use of Q-Sepharose Fast Flow (FF) columns with different volumes (1, 10 and 40 ml) for the preparative purification of supercoiled plasmid DNA. Plasmid yields, column loadings, binding conditions and fraction volumes are reported. Final product quality is assessed by gel electrophoresis, restriction analysis and transformation experiments. Q-Sepharose is a strong anion-exchanger with quaternary amine groups bound to 6% highly crosslinked agarose particles with a mean diameter of 90 μm. The structure of this material combines relatively large voids into which large molecules can penetrate, with dense matrix regions containing extensively aggregated agarose double helices in a side-by-side assembly [20]. The crosslinking locks the agarose chains together stabilizing the structure and increasing its rigidity [21]. According to the manufacturer, the exclusion limit for Q-Sepharose FF is $4 \cdot 10^6$ for globular proteins (≈1870 Å diameter). The resin has been reported by the manufacturer [14] and others [10] as capable of separating open circular from supercoiled plasmid.

A perfusion Poros anion-exchange column also is used in this work for analytical purposes. Poros 20 QE is a polystyrene–divinylbenzene support coated with crosslinked polyethyleneimine groups. This media combines large ''throughpores'' with diameters of 6000–8000 Å interconnected with smaller diffusive pores with mean diameter of 500–1000 Å. The accessibility of the internal volumes of Poros materials has been measured and predicted with a network model by Loh and Wang [22], who report exclusion coefficients lower than 0.2 for spherical particles with diameters higher than 2000 Å ($4.5 \cdot 10^6$).

A small plasmid, pUC18 [carrying the gene for the α-peptide of lac Z (β-galactosidase)] with 2686 base pairs (bp) and a molecular mass of 1 772 760 was chosen as a model vector. Its size is close to the size of *E. coli* high-molecular-mass RNAs such as ribosomal RNA and messenger RNA. Some rough estimates of the dimensions of plasmid pUC18 can

be helpful for the understanding of the anion-exchange process. The average length of the DNA chain of a nicked or open circular pUC18 molecule is 9000 Å (the plasmid size in base pairs, 2686, times 3.35 Å/bp) and if these plasmid forms were to assume the shape of a circle, the corresponding diameter would be 2864 Å. Upon supercoiling, plasmids adopt a branched interwound shape and become more compact and uniform. This structure is thought to be highly dynamic, with branches forming and retracting randomly [7]. The dimensions of the resulting superhelix will be a function of the number of times the two strands of the DNA double helix are intertwined. For a typical degree of supercoiling and extrapolating the results presented by Boles et al. [7] for 3.5 and 7.0 kb plasmids to pUC18, the superhelix axis should be close to 3689 Å and the superhelix diameter to 113 Å (see Appendix A).

2. Experimental

2.1. General

2.1.1. Materials

Luria broth (LB) was from Difco Labs. (Detroit, MI, USA) and Q-Sepharose from Pharmacia (Piscataway, NJ, USA). *E. coli* subcloning efficiency DH5α competent cells, plasmids pUC18 and pSPORT 1 and molecular mass marker *Hind III* digest from lambda phage DNA were from Gibco-Life Technologies (Rockville, MD, USA). Restriction endonuclease *Ssp I* was from New England Biolabs (Beverly, MA, USA), RNase A from Sigma (St. Louis, MO, USA) and *S1* and mung bean nucleases from Pharmacia (Piscataway, NJ, USA). All salts were analytical grade.

2.1.2. Equipment

Analytical chromatography was performed with a Beckman (Fullerton, CA, USA) System Gold high-performance liquid chromatography (HPLC) system (diode array detector module 168, programmable solvent module 126, System Gold software). A Pharmacia fast protein liquid chromatography (FPLC) system (P500 pump, LCC 500 chromatographic controller, single path UV-1 monitor with 3 mm path length cell) was used for the preparative purification of plasmid. Injection of samples was performed using either a 1-ml loop or a 10-ml superloop. Agarose gels were run in a quick-screening horizontal gel electrophoresis unit (QSH) from IBI (New Haven, CT, USA) coupled to a Pharmacia EPS 200 power supply.

2.2. Methods

2.2.1. Transformation experiments

E. coli DH5α competent cells were transformed with plasmid pUC18 or pSPORT 1 (Gibco-Life Technologies) using a standard method [23]. The relative transformation efficiencies of the different plasmid fractions were determined by plating the transformed bacteria on LB plates containing 100 μg/ml ampicillin [23]. LB plates with Xgal/IPTG [23] were also used to check for plasmid integrity.

2.2.2. Bacterial culture

E. coli cultures were grown (LB medium, 100 μg/ml ampicillin) overnight at 37°C in 100-ml shaker flasks at 250 rpm. Larger volume cultures (up to 250 ml) were inoculated with the appropriate amount of the overnight culture and incubated under the same conditions. Bacteria were harvested at late log phase (A_{600} approx. 4.5–5.0).

2.2.3. Lysis and primary plasmid isolation

Bacteria were lysed using a modification of the alkaline method [24] as described in Ref. [5]. The procedure is described next for a reference broth volume of 100 ml, although larger volumes (up to 3 l) were used at times. Cells were centrifuged at 10 000 *g* for 30 min and supernatants discarded. The bacterial pellets were resuspended in 10 ml of 61 m*M* glucose, 10 m*M* Tris, 10 m*M* EDTA, pH 8.0. Lysis was performed at room temperature by adding 20 ml of a 200 m*M* NaOH, 1% sodium dodecyl sulfate (SDS) solution. Cellular debris, cDNA and proteins were precipitated by gently adding and mixing 15 ml of 3 *M* potassium acetate pH 5.0 prechilled to 4–10°C. The precipitated material was removed by filtration through four layers of cheesecloth followed by filtration through analytical filter paper in order to remove small particulate material. Precipitation of plasmid was carried out for 2 h at

room temperature by adding 0.6 volumes of isopropanol. After centrifugation at 10 000 *g*, the pellets were ressuspended in 10 m*M* Tris, 1 m*M* EDTA, pH 8.0 buffer. At this stage, high-molecular-mass RNA was cleaved using RNase A (20 μg/ml) for 30 min at 37°C. Next, ammonium acetate was dissolved in the plasmid preparation up to a concentration of 2.5 *M* followed by 15 min incubation on ice. Precipitated proteins were removed by centrifugation at 10 000 *g* for 20 min. Plasmid was finally precipitated with isopropanol (0.6 volumes) for 2 h at room temperature, centrifuged at 10 000 *g* and resuspended in 1 ml 10 m*M* Tris, 1 m*M* EDTA, pH 8.0 buffer. Total ''native'' plasmid (sc and oc) was quantified by HPLC.

2.2.4. Plasmid miniprep

Plasmid standards were prepared using the QIAGEN (Hilden, Germany) plasmid mini kit according to the instructions of the manufacturer. DNA concentration was measured in a Hewlett-Packard (Waldbronn, Germany) 8452A diode array spectrophotometer at 260 nm ($A_{260}=1$ corresponds to 50 μg DNA/ml).

2.2.5. Agarose gel electrophoresis

Plasmid and DNA fragments were analyzed by electrophoresis using 7 cm, 1% agarose (Sigma, St. Louis, MO, USA) gels. Running buffer was a 40 m*M* Tris base, 20 m*M* sodium acetate, 2 m*M* EDTA, pH 8.3 solution and electrophoresis was carried out at 65 V for 1 h. Whenever deemed necessary, samples were precipitated with isopropanol (0.7 volumes), centrifuged at 15 000 *g* for 30 min and resuspended in 10 μl of 10 m*M* Tris, 1 m*M* EDTA pH 8.0 buffer. After electrophoresis gels were stained for 1 h with ethidium bromide (5 μg/ml) and then visualized and photographed under UV light.

2.2.6. Restriction endonuclease and nuclease digestion

Fractions from the preparative runs were precipitated as described in Section 2.2.5 and ressuspended either in *Ssp I* or nuclease assay buffers. Samples were incubated at 37°C for 1 h after *Ssp I* addition, and at 37°C for 10 min after nuclease *S1* or mung bean nuclease addition.

2.2.7. Protein analysis

A micro-BCA (bicinchoninic acid) assay from Pierce (Rockford, IL, USA) was used to measure protein content.

2.3. Analytical chromatography

2.3.1. Column

A polyether ether ketone (PEEK) column with 10 cm×0.46 cm I.D. and a bed volume of 1.7 ml was packed with 20-μm particles of Poros 20 QE strong anion-exchanger from Perseptive Biosystems (Framhingham, MA, USA) using the Poros Self Packing Device according to the instructions of the manufacturer. Poros 20 QE is a polystyrene–divinylbenzene support coated with crosslinked polyethyleneimine groups.

2.3.2. Mobile phase

Room temperature gradient elution with increasing salt concentration was used. Buffer A was 10 m*M* Tris, 1 m*M* EDTA, pH 8.0 and buffer B 10 m*M* Tris, 1 m*M* EDTA, pH 8.0, 2 *M* NaCl. Salt concentration was 0.5 *M* for the first 2 min followed by a 5 min linear gradient from 0.5 *M* to 2.0 *M*. Salt concentration was held at 2.0 *M* for 2 min and then decreased to the initial value of 0.5 *M*. The flow-rate was 2 ml/min and absorbance was monitored at 260 nm. Injection volumes were between 50 and 200 μl. The column was periodically cleaned with 1 *M* NaOH followed by 2 *M* NaCl.

2.4. Preparative chromatography

2.4.1. Columns

Columns HR5/5 (5.0 cm×0.5 cm I.D., $V_{bed}=1$ ml), HR16/10 (5.0 cm×1.6 cm I.D., $V_{bed}=10$ ml) and XK50/20 (2.0 cm×5.0 cm I.D., $V_{bed}=40$ ml) from Pharmacia (Piscataway, NJ, USA) were packed according to the manufacturer with Q-Sepharose Fast Flow, a strong anion exchanger with quaternary amine groups bound to 6% highly crosslinked agarose particles (90 μm).

2.4.2. Mobile phase

With the HR5/5 column buffer A was 10 m*M* Tris, 1 m*M* EDTA, pH 8.0 and buffer B 10 m*M* Tris, 1 m*M* EDTA, pH 8.0, 2 *M* NaCl. With columns

HR16/10 and XK50/ buffer A was 10 m*M* Tris, 1 m*M* EDTA, pH 8.0, 600 m*M* NaCl and buffer B 10 m*M* Tris, 1 m*M* EDTA, pH 8.0, 700 m*M* NaCl. The absorbance of the eluate was measured at 254 nm and separations were carried out in a cold room at 4°C.

Two gradients were used with the HR5/5 (1 ml) column: gradient 1, 620 m*M* for 20 min, 620–700 m*M* in 32 min, 700–800 m*M* in 5 min, 800 m*M* for 5 min; gradient 2, 560 m*M* for 20 min, 560–700 m*M* in 28 min, 700–800 m*M* in 5 min, 800 m*M* for 5 min. Flow-rate was 0.5 ml/min and injection volume was 1 ml.

The following gradients were used with the HR16/10 (10 ml) column: gradient 3, 645 m*M* for 20 min, 645–700 m*M* in 22 min, 700 m*M* for 10 min; gradient 4, 645 m*M* for 20 min, 645–672.5 m*M* in 11 min, 672.5–700 m*M* in 0.1 min and 700 m*M* for 14 min. Flow-rate was 5 ml/min.

A single gradient was used in the XK50/2 (40 ml) column: gradient 5, 645 m*M* for 42 min, 645–676 m*M* in 26 min, 676–700 m*M* in 0.2 min and 700 m*M* for 32 min. Flow-rate was 10 ml/min. Each peak obtained in the preparative runs was collected as a single fraction and kept for HPLC, protein, gel electrophoresis and restriction analysis.

2.4.3. Column cleaning

After each run, columns were cleaned with 15 column volumes of a 1 *M* sodium hydroxide solution, followed by 15 column volumes of buffer B. Equilibration was then performed with the appropriate starting buffer until constant UV baseline was obtained.

3. Results

3.1. Analytic chromatography

Standards of plasmid pUC18 (2.7 kilobase pairs, kbp) prepared using the Qiagen miniprep kit, were injected (50–350 μl) in the analytical Poros column and used to construct a calibration curve. A typical chromatogram is shown in Fig. 1a). Characteristic features of the chromatogram are the first peak at 0.7 min, which corresponds to the sample buffer (10 m*M* Tris, 1 m*M* EDTA, pH 8.0, 0 *M* NaCl) and the

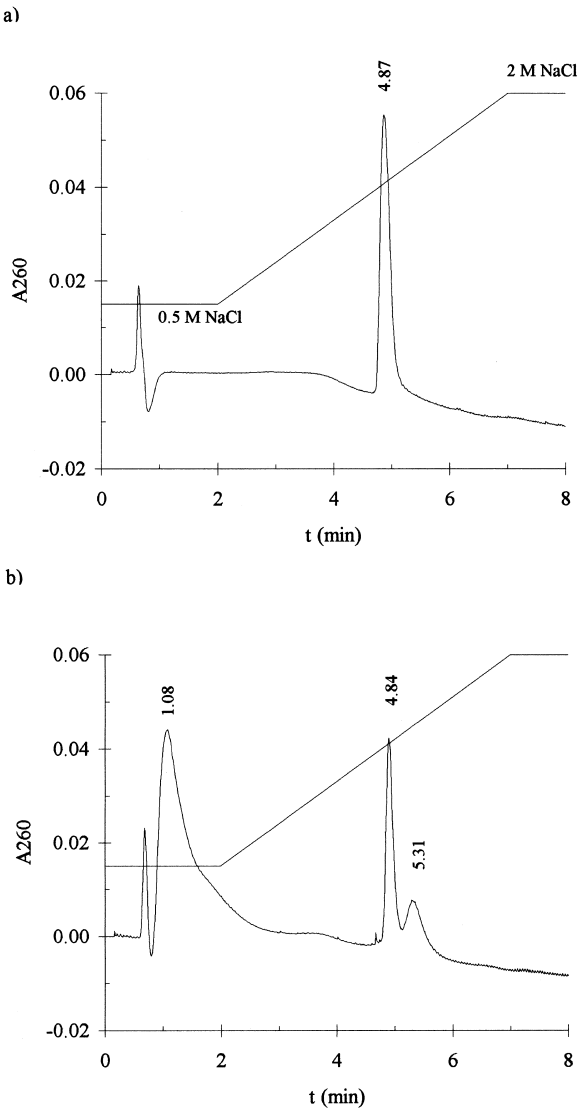

Fig. 1. (a) HPLC analytical chromatogram (1.2 μg pUC18) and (b) analysis of plasmid preparation P1 (1.1 μg of supercoiled and open circular pUC18).

drifting baseline caused by the increasing ionic strength of the eluent. The retention time of the plasmid peak was usually in the range 4.84–4.88 min. Taking into account a delay of 2.5 min between the pumps and the detector, this corresponds to an ionic strength around 611 m*M*. Under the conditions used, the Poros column was not able to resolve open circular, supercoiled and *Ssp I* linearized plasmid. Furthermore, when samples of either the molecular

mass marker λ DNA *Hind III* digest (fragments with 0.6, 2.0, 2.3, 4.4, 6.6, 9.4 and 23 kbp) or of the plasmid pSPORT 1 (4.1 kbp) were injected onto the column, single peaks with the exact same shape and retention time as pUC18 were obtained. In spite of this inability to separate double-stranded DNA in the molecular mass range 0.6–23 kbp, the Poros column was found suitable for a fast and reproducible quantification of total (oc+sc) plasmid DNA. An eight point calibration curve (0–0.7 μg) was generated, yielding a linear relationship, $A_{260}=6.8131\cdot$ DNA (μg), with a correlation coefficient 0.999.

3.2. Primary isolation

Two plasmid solutions, hereafter named P1 and P2, were prepared according to the procedure described in Section 2.2.3 and used as feedstock for the three preparative columns. The amount of ''native'' plasmid was estimated by HPLC (P1, 570 μg/ml, P2, 1088 μg/ml) and protein was assayed by the BCA test (P1, 26.3 μg/ml, P2, 94.2 μg/ml). Fig. 1b shows the chromatogram obtained for preparation P1. Apart from plasmid, two additional peaks are present in the chromatogram. The broad peak with a maximum at 1.08 min corresponds to cell proteins and low-molecular-mass RNA and oligoribonucleotides which are obtained after RNase A digestion. The second peak (5.31 min), partially overlapping with the plasmid was identified as described next, as a denatured form of plasmid.

Analysis by gel electrophoresis (Fig. 2) showed that the material in the 5.31 min peak (lane 7) migrates with the apparent size of a 1.73 kbp linear fragment. This is slightly higher than the apparent size of the ''native'' supercoiled plasmid (1.66 kbp) variant (lane 3). The fluorescent intensity of this band upon ethidium bromide staining was found to be very low in comparison with the intensity usually obtained with the open circular and supercoiled forms, which meant that higher amounts, as measured by absorbance at 260 nm, had to be used for detection in electrophoresis. Contrary to the supercoiled and open circular forms, which readily undergo digestion with the endonuclease *Ssp I*, yielding linear plasmid as a single band (lane 4), the denatured plasmid (d) was found to be recalcitrant to digestion with the same amounts of *Ssp I* (lane 8).

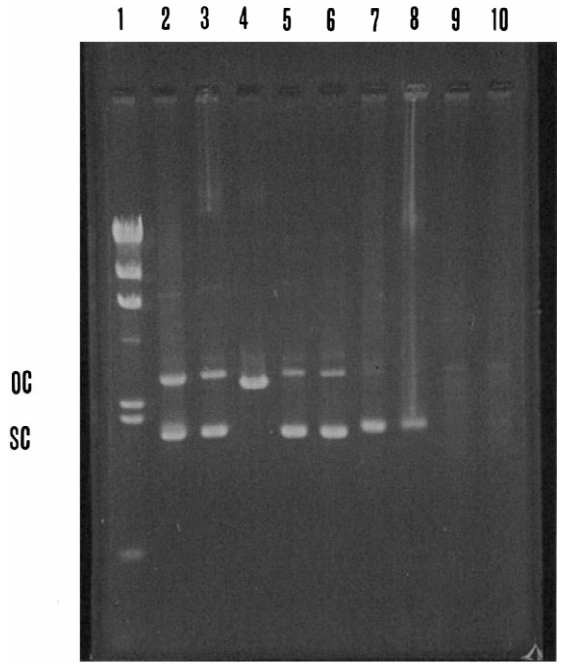

Fig. 2. Analysis of HPLC peaks by 1% gel electrophoresis: molecular mass marker (lane 1) and plasmid preparation P1 (lane 2). The supercoiled and open circular plasmid eluting at 4.84 min in HPLC (lane 3) was subjected to digestion with *Ssp I* (lane 4), nuclease *S1* (lane 5) and mung bean nuclease (lane 6). The denaturated plasmid eluting at 5.32 min in HPLC (lane 7) was also treated with *Ssp I* (lane 8), nuclease *S1* (lane 9) and mung bean nuclease (lane 10).

On the other hand, when the single-stranded DNA specific mung bean and *S1* nucleases were incubated with the denatured plasmid, the original band disappeared entirely, indicating the presence of large amounts of single-stranded DNA (lanes 9 and 10). Both nucleases are unable to digest double-stranded DNA as shown in Fig. 2 with the supercoiled and open circular forms of pUC18 (lanes 5 and 6).

The above findings indicate that the denatured plasmid consists of a compact covalently closed, supercoiled form which carries large stretches of single-stranded DNA. This form of plasmid was able to transform *E. coli* competent cells with a transformation efficiency of $9.5\cdot10^3$ transformants/μg DNA. Denatured plasmid forms with similar properties, except for lower apparent sizes, have been described [25–27] and are usually associated to the alkaline lysis based purification procedure. In fact,

by exposing supercoiled plasmid DNA to harsh alkaline conditions we were able to prepare a denatured form of plasmid with similar HPLC and electrophoresis properties (results not shown).

3.3. Preparative chromatography

3.3.1. Scouting

The goal of the preparative ion-exchange chromatography in the downstream processing is the elimination of low-M_r RNA and denatured plasmid from the preparation. A small column (HR5/5, 1 ml) was first used to establish and optimize the separation. Fig. 3 shows two chromatograms corresponding to 22 μg plasmid loadings of preparation P1, obtained with the two different gradients 1 and 2.

In the first separation (Fig. 3a), three peaks were obtained. HPLC analysis (Fig. 4a) showed that the first peak consisted mainly of low-M_r RNA but two plasmid forms (supercoiled and denatured) also were present as evidenced by the two overlapping peaks obtained in the 4.8–5.3 min region. The plasmid material in this fraction was detected by gel electrophoresis as a band with an apparent size equal to ''native'' supercoiled plasmid (lane 3, Fig. 5). Part of it was found to be resistant to digestion with *Ssp I* endonuclease (lane 4), which confirms the presence of the denatured form in the flow-through. The second peak in the preparative chromatogram contained mainly open circular plasmid (Fig. 4b) as shown by electrophoresis (lane 5). This form was readily cleaved by *Ssp I* endonuclease, yielding linear plasmid which migrates slightly faster (lane 6). The last fraction from the preparative column contained most of the plasmid in the preparation (Fig. 4c) as a supercoiled form (lane 7) amenable to digestion with *Ssp I* (lane 8).

Different plasmid loadings were tested in an attempt to maximize column productivity and check if the presence of some supercoiled plasmid in the flow-through could be attributed to overloading. Table 1 shows the results of the HPLC analysis on the open circular and supercoiled plasmid fractions. The plasmid yield, calculated on the basis of ''native'' plasmid injected, obtained in each fraction was found to be independent of the amount of plasmid loaded on the column. An average of 10.3% of the total injected plasmid was recovered in the open

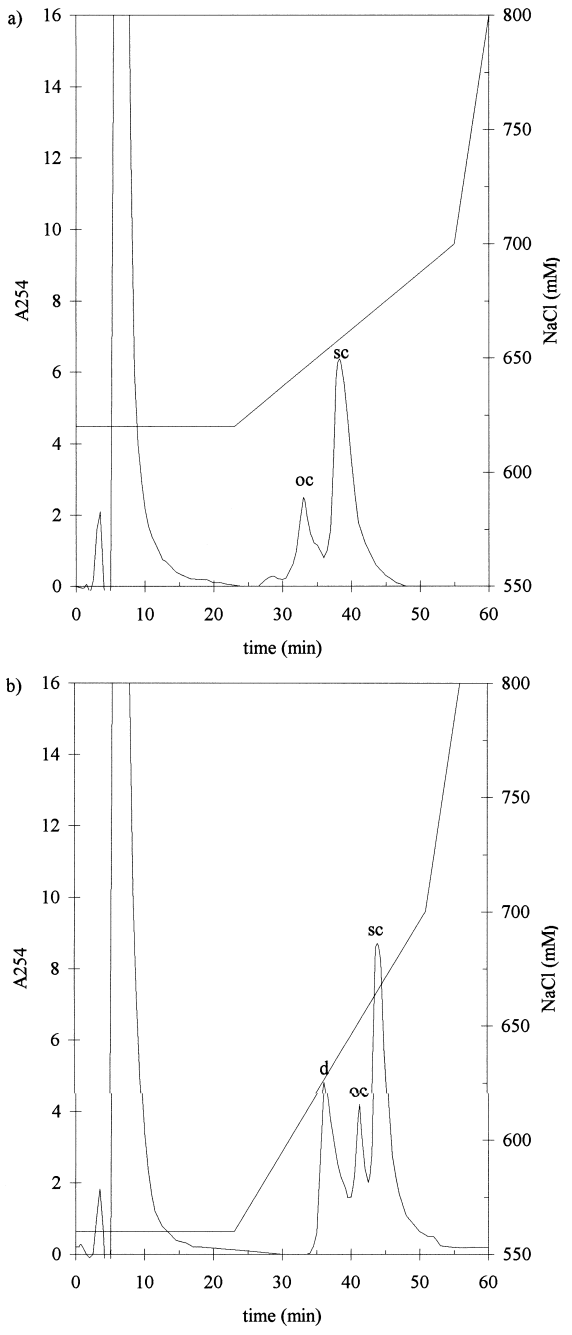

Fig. 3. FPLC purification with the 1 ml column (HR5/5 column, 22 μg loading of total ''native'' plasmid, preparation P1, flow-rate 1 ml/min): (a) gradient 1, (b) gradient 2.

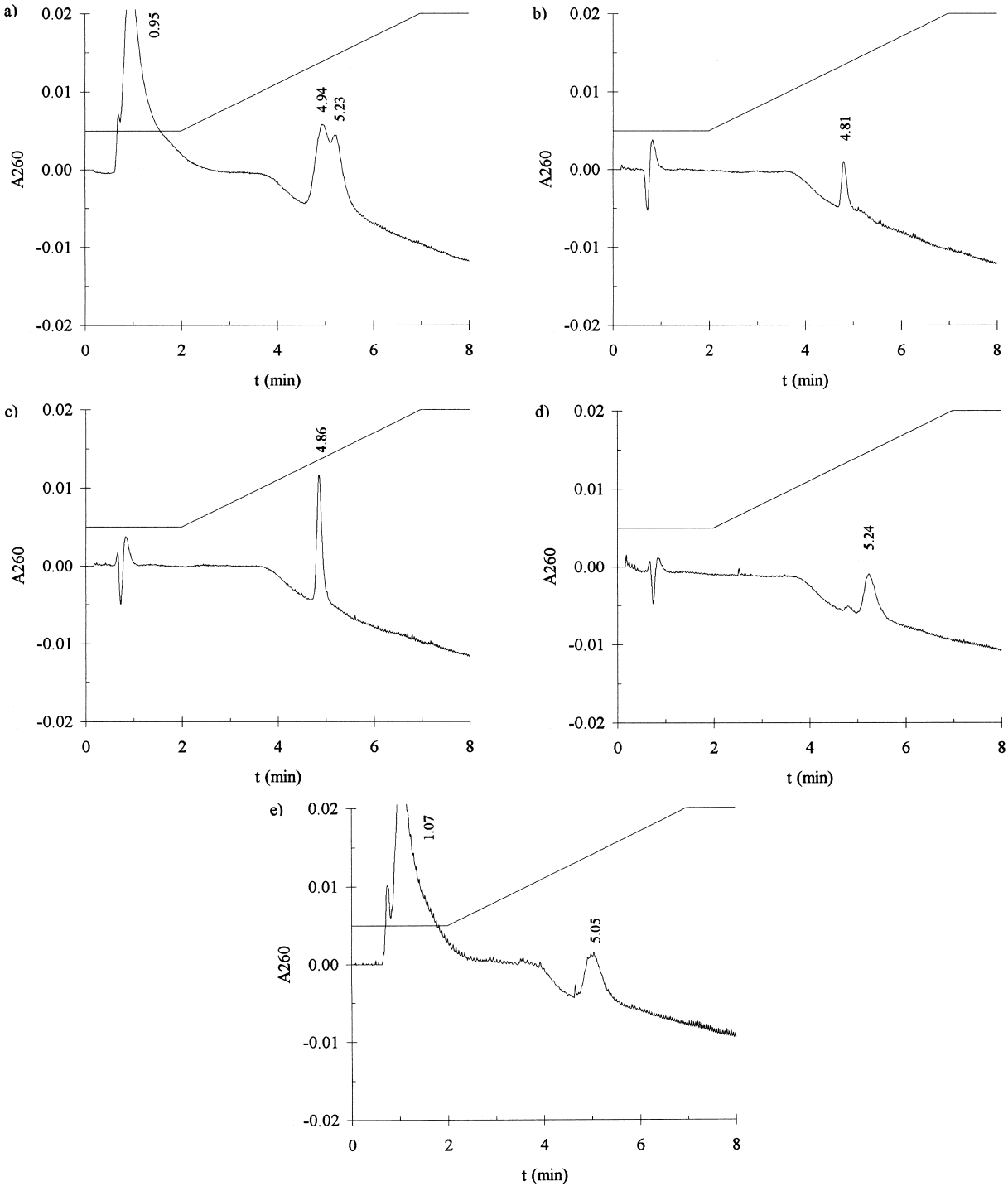

Fig. 4. HPLC analysis of fractions obtained from the preparative runs shown in Fig. 3 (HR5/5 column, 22 μg loading of total ''native'' plasmid, preparation P1). Gradient 1 (Fig. 3a): (a) flow-through, (b) open circular fraction, (c) supercoiled fraction. Gradient 2 (Fig. 3b): (d) denatured plasmid fraction, (e) flow-through.

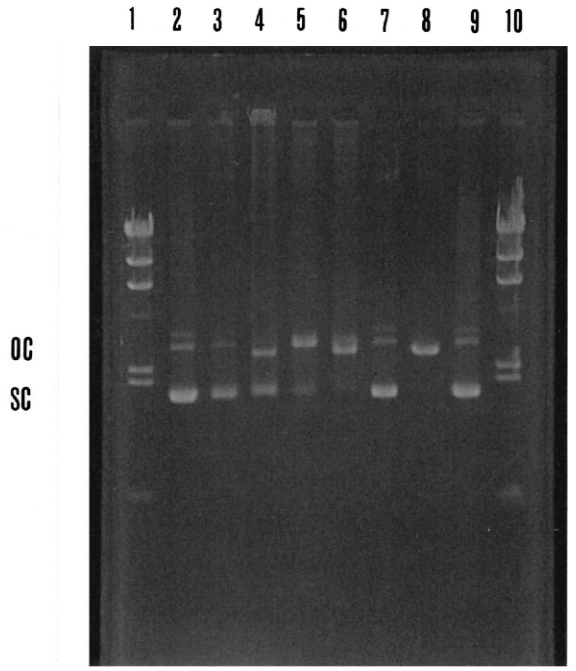

Fig. 5. Gel electrophoresis analysis of FPLC fractions from the preparative run shown in Fig. 3a: lanes 1 and 10: molecular mass marker. Lanes 2 and 9: feed, plasmid preparation P2. Lane 3: denaturated and supercoiled plasmid in the flow-through. Lane 4: material in the flow-through after digestion with *Ssp I*. Lane 5: open circular plasmid fraction. Lane 6: open circular fraction after digestion with *Ssp I*. Lane 7 supercoiled plasmid fraction. Lane 8: supercoiled fraction after *Ssp I* digestion.

circular fraction and an average of 55.4% on the supercoiled fraction, corresponding to a total plasmid yield of 65.7%. The proportion of recovered oc to sc plasmid also was constant and around 16%. Surprisingly, supercoiled plasmid was always present in the flow-through, even for the lower loadings.

In order to improve the plasmid yield, the initial loading of the column was carried out at a lower ionic strength (560 m*M* vs. 620 m*M*) and a sharper gradient was used to elute the plasmid (Fig. 3b). One major difference was observed: an extra early eluting peak appeared which was identified by HPLC (Fig. 4d) and electrophoresis as being the denatured plasmid form, indicating that it is now binding to the resin instead of being washed away in the flow-through as previously. However, supercoiled plasmid was still obtained in the flow-through as seen in the HPLC (Fig. 4e) chromatogram which now shows the presence of just one peak in the 4.8–5.3 region. The shape of this peak however is slightly different from the typical, sharp peaks of pure plasmid.

The second half of Table 1 shows the results obtained with this new gradient for different plasmid loadings. A first observation confirms that the sharper gradient lead to smaller and more concentrated plasmid fractions, as expected. Again the yields of plasmid obtained in each fraction were found to be independent of the loading. More strikingly, the yields obtained in each fraction were

Table 1
Purification of supercoiled plasmid with the 1-ml column

Gradient	Load[a] (μg)	V_{inj} (ml)	OC fraction		SC fraction		Yields (%)		
			Vol. (ml)	pDNA (μg)	Vol. (ml)	pDNA (μg)	OC	SC	Total
1	10.6	1.0	2.6	1.52	5.4	5.76	14.4	54.6	69.0
1	19.5	1.0	3.4	1.96	5.3	11.5	10.0	58.8	68.8
1	21.6	1.0	3.3	2.49	6.0	12.4	11.5	57.3	68.8
1	22.5	1.0	2.4	2.38	6.5	13.1	10.6	58.4	69.0
1	26.6	1.0	3.3	2.74	6.6	15.0	10.3	56.5	66.8
1	37.1	1.0	2.9	3.05	8.7	20.5	8.2	55.2	63.4
1	46.5	1.0	3.1	3.34	9.2	21.7	7.2	46.7	53.9
2	10.6	1.0	1.4	1.09	3.2	6.04	10.3	57.3	67.6
2	21.0	1.0	1.4	1.82	4.5	11.6	8.7	55.5	64.2
2	21.6	1.0	1.6	2.03	4.4	11.5	9.4	53.4	62.8
2	21.6	1.0	1.4	1.70	5.4	10.6	7.9	49.4	57.2
2	26.6	1.0	1.7	3.15	5.6	14.7	11.9	55.3	67.2
2	30.7	1.0	1.5	2.36	8.7	17.0	7.7	55.5	63.1
2	46.3	1.0	1.5	3.17	5.4	25.0	6.8	53.9	60.8

[a] ''Native'' plasmid, preparation, P1.

identical to the ones obtained with the previous gradient: 8.9% for the open circular fraction and an average of 54.3% for the supercoiled fraction which corresponds to a total plasmid yield of 63.3%.

3.3.2. Scale-up

Based on the previous results, the process was scaled-up 10 and 40 times. Fig. 6a shows a separation carried out in the 10-ml column (140 μg loading, preparation P1, gradient 4) and Fig. 6b a separation from the 40-ml column (649 μg loading, preparation P2, gradient 5). Gradient 1, used with the 1-ml column (Fig. 3a) was reproduced in the larger columns with some slight modifications. For instance, a salt step was included right after the elution of the open circular peak. This fine tuning of the gradient reduced the volume and increased the concentration in the supercoiled plasmid fraction – sharper peaks were obtained. The superficial velocity of the eluent was maintained when scaling from the 1-ml column to the 10-ml one. However, due to limitations in the FPLC system, it was necessary to reduce the velocity to half when operating the 40-ml column. This explains the two-fold difference in the time scales of Fig. 6a Fig. 6b. The difference in the relative size of oc to sc plasmid peaks in both chromatograms is a consequence of the fact that two difference preparations were used as feed for the two columns. Preparation P1 had a higher content of oc plasmid than preparation P2. This is clearly seen by comparing the relative intensities of the oc and sc bands obtained by gel electrophoresis: P1, Fig. 2, lane 2 and P2, lane 2, Fig. 5.

Table 2 shows the results obtained in several runs carried out with different plasmid loadings in the 10-ml column. Results obtained with a gradient (3) which does not including the final, sharpening salt step are also presented. The concentration effect arising from the inclusion of this salt step in gradient 4 is evidenced by the lower volumes of the sc fractions. However, average yields of sc and total ''native'' plasmid were slightly lower in this case (67.7% vs. 73.8% for sc and 77.9 vs. 82.6% for total plasmid). The 40-ml column also was loaded with different amounts of plasmid (Table 3). Average yields were 64.3% for sc and 2.6% for oc plasmid, which corresponds to a total ''native'' plasmid yield of 66.8%. As in the 1-ml column, the plasmid

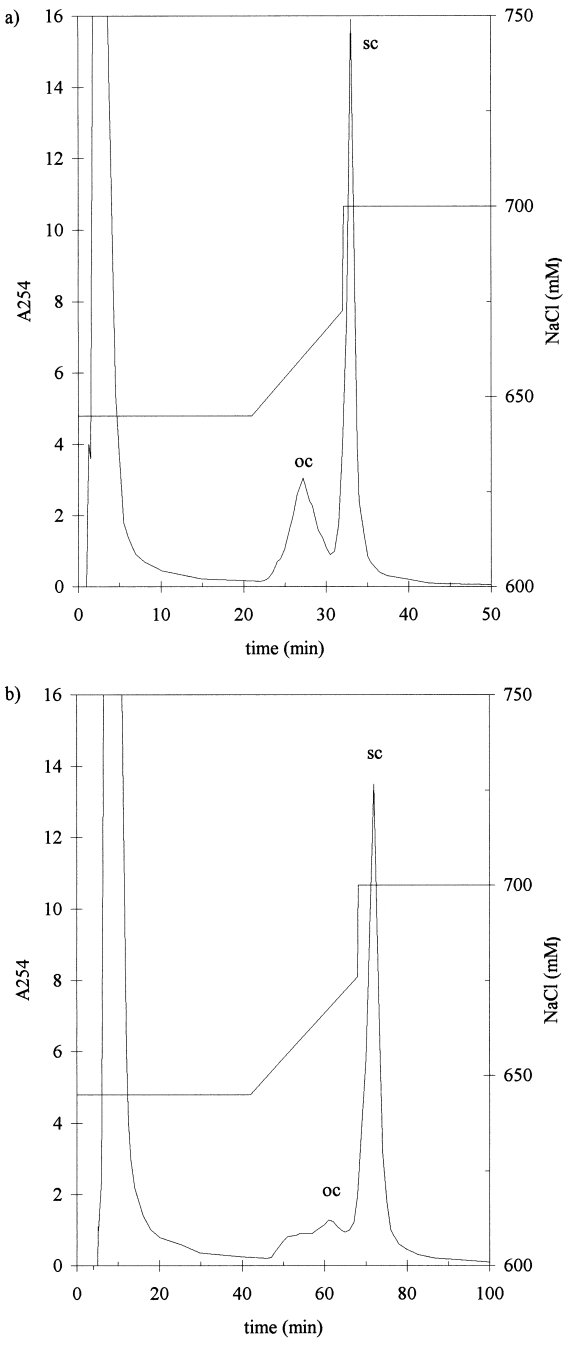

Fig. 6. Scale-up of anion-exchange chromatography: (a) 10 ml column, 140 μg loading of total ''native'' plasmid, preparation P1, flow-rate 5 ml/min and (b) 40 ml column, 649 μg loading of total ''native'' plasmid, preparation P2, flow-rate 10 ml/min.

Table 2
Purification of supercoiled plasmid with the 10-ml column

Gradient	Load[a] (μg)	V_{inj} (ml)	OC fraction		SC fraction		Yields (%)		
			Vol. (ml)	pDNA (μg)	Vol. (ml)	pDNA(μg)	OC	SC	Total
3	106.3	2.5	42.5	10.1	48.0	73.2	9.5	68.9	78.4
3	167.4	5.0	44.0	15.1	53.9	118.9	9.0	71.0	80.0
3	251.1	7.5	40.5	21.7	62.5	181.9	8.6	72.4	81.1
3	334.8	10.0	40.0	28.8	79.0	259.4	8.6	77.5	86.1
3	425.0	10.0	38.5	33.1	75.0	337.6	7.8	79.4	87.2
4	106.3	2.5	44.0	10.8	18.0	65.3	10.2	61.5	71.6
4	140.3	3.5	41.0	15.5	40.0	102.6	11.1	73.1	84.2
4	200.5	5.0	40.0	20.5	41.5	131.8	10.2	65.7	76.0
4	200.5	5.0	38.0	23.1	43.5	140.7	11.5	70.2	81.7
4	297.5	7.0	42.5	26.2	49.0	196.3	8.8	66.0	74.8
4	360.9	9.0	38.5	35.6	55.0	250.6	9.9	69.4	79.3

[a] ''Native'' plasmid, preparation, P1.

Table 3
Purification of supercoiled plasmid with the 40-ml column

Gradient	Load[a] (μg)	V_{inj} (ml)	OC fraction		SC fraction		Yields (%)		
			Vol. (ml)	pDNA (μg)	Vol. (ml)	pDNA (μg)	OC	SC	Total
5	324.5	5.0	100	93.0	126	211.8	2.8	65.3	68.0
5	649.0	10.0	130	19.1	170	440.7	2.9	67.9	70.8
5	857.0	10.0	142	25.3	160	509.4	3.0	59.4	62.4
5	1284	10.0	128	26.4	204	785.0	2.1	61.1	63.2
5	1500	10.0	102	33.6	223	1014.2	2.2	67.6	69.8

[a] ''Native'' plasmid, preparation, P2.

recovery from both columns was not affected by increasing loadings.

Fig. 7 summarizes the results obtained with the three columns, presenting the yield of plasmid isolated in the supercoiled fractions as a function of the specific column loading, i.e., amount of total ''native'' plasmid loaded per ml of gel. Yields were higher with the 10-ml column and lower with the 1-ml one. Overall, the plot shows that, apparently, column size had no influence in the performance of the process, as measured by sc plasmid yield. The 8% standard deviation in an average yield of 62.0% can be attributed to process variability.

3.3.3. Column cleaning

Although the primary isolation procedure used to recover plasmid may remove most of the host cell

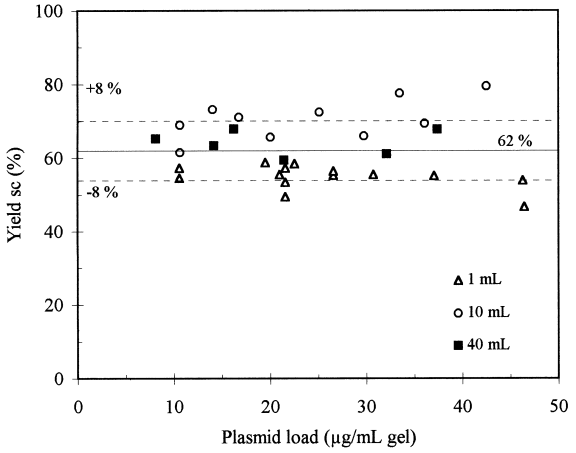

Fig. 7. Yield of plasmid obtained in the supercoiled fractions collected from the three anion-exchange columns.

cDNA, it is likely that some large cDNA fragments are still present in the feed which is introduced in the ion-exchange columns. But none of the fractions which eluted during the operation of the columns was found to contain cDNA (as checked by gel electrophoresis). However, when cleaning the columns with the procedure described in Section 2.4.3, it was found that some UV absorbing material eluted with the 1 *M* NaOH solution. This material, which can only be removed from anion-exchange columns after NaOH treatment is cDNA, as identified by other authors [15].

3.3.4. Plasmid quality

The quality of the plasmid isolated in the late eluting fraction of the preparative columns (Figs. 3 and 6) was tested by performing HPLC analysis, gel electrophoresis, restriction analysis, transformation experiments and protein assays. HPLC was particularly useful in quantifying total ''native'' plasmid (sc+oc) and testing for low-M_r RNA and denatured plasmid contamination (Fig. 4). With gel electrophoresis the homogeneity of the final plasmid in terms of size and structure was assessed, clearly indicating the isolation of supercoiled forms from other plasmid variants (Fig. 5). Plasmid identity was confirmed by restriction analysis with the restriction enzyme *Ssp I*. Both open circular and supercoiled plasmid variants were readily digested with *Ssp I*, yielding a single band with an apparent size of 2.86 kbp (Fig. 5). In contrast, most of the plasmid present in the flow-through fraction was found to be recalcitrant to cleavage by *Ssp I*. Protein contamination was assayed using the BCA test. No protein was detected in the open circular or supercoiled plasmid fractions.

The plasmid in the open circular and supercoiled fractions was used to transform competent DH5α cells. The mean transformation efficiency obtained with the plasmid isolated from the 40-ml column was $6.51 \cdot 10^6$ transformants/μg for the oc and $11.7 \cdot 10^6$ transformants/μg for the sc forms. Both variants produced ampicillin resistant clones, but with higher efficiencies being obtained with the supercoiled plasmid. The plasmid in the flow-through was capable of transforming cells; efficiencies were not determined in this case due to the difficulty in determining the total plasmid amount in this fraction. The transformed bacteria were plated on Xgal/IPTG indicator plates. Blue transformants were always obtained, indicating that the gene for the α-peptide of lac Z (β-galactosidase) in pUC18 is intact.

4. Discussion

Denatured plasmid forms, similar to the one identified in this work as one of the major contaminants in the process streams, have been described in the literature. It is known that alkaline lysis above pH 12.5 can irreversibly denature plasmids by disrupting base pairs that should remain in register to serve as nuclei for complete renaturation during the subsequent neutralization with potassium acetate [25]. This disruption and translocation of the important base pairs may cause the plasmid to form incongruent complementary base pairs or cruciform loops upon neutralisation, resulting in an irreversibly denatured, covalently closed plasmid containing large regions of highly twisted single-stranded material. The single-stranded regions are certainly richer in the relatively weak AT base pairs, while the remaining double-stranded regions should have a high content of the much stronger GC base pairs. The compactness of the denatured form identified in this work, which allows it to migrate in a gel with approximately the same velocity as the ''native'' supercoiled plasmid, is probably associated to same extent to the strong tendency of single-stranded DNA to fold back on itself forming irregular double-helical hairpin loops [28]. Measurement of the pH after addition of the lysis solution confirmed that the buffer capacity of the solution used to resuspend the cells (61 m*M* glucose, 10 m*M* Tris, 10 m*M* EDTA, pH 8.0) [5] was not enough to maintain the pH in the 12.0–12.5 region as recommended [25] – with the volumes used, pH increased to 13.5. Therefore, the presence of the denatured plasmid was attributed to the harsh alkaline conditions used during lysis.

The native and denatured plasmid forms exhibited different elution patterns in the two strong anion-exchange resins used in this work. The analytical Poros column which was found unable to separate double-stranded DNA molecules of different base

composition, structure and size, hence overall net charge, could nevertheless clearly separate two plasmid forms (native and denatured supercoiled) which differ only in the relative amount of double and single-stranded DNA. The presence of single strands of DNA increased the binding to the Poros column, suggesting that more negative sites in the molecule were interacting with the anion exchanger groups. When changing from the analytical Poros resin to the preparative Q-Sepharose material an inversion of the elution pattern of the plasmid forms was observed, with the denatured plasmid form eluting before the oc and sc variants. This indicates less interaction of the denatured plasmid with the anion exchanger groups. Another plausible explanation for the elution order inversion when switching between Q-Sepharose and Poros could be the additional presence of hydrophobic interactions, explained as follows. The crosslinked agarose support of Q-Sepharose presents an extremely hydrophilic surface while the base Poros bead, made of polystyrene–divinylbenzene, is very hydrophobic. Although a hydrophilic polymer (polyethyleneimine) is used as a coating in the Poros material, this may not completely shield the hydrophobic nature of the bead. Thus, the denatured plasmid (with more single-stranded DNA) which presents a more hydrophobic surface than the native (oc and sc) plasmid due to the presence of exposed bases, may interact with the more hydrophobic Poros support. This would lead to longer retention times on Poros beads due to this additional binding mechanism as compared to the more hydrophilic Q-Sepharose.

In spite of the above mentioned hypothesis, at this stage there is no clear indication on the reasons why the same two plasmid forms exhibit opposite elution patterns on the two strong anion exchangers. Nevertheless, as the size of plasmid molecules is very close to the exclusion limits of the two resins tested, it is probable that plasmid size/shape together with pore structure is playing an important role in the retention mechanism.

Although the data on the exclusion limits of Poros (≈2000 Å) and Q-Sepharose (≈1900 Å) pores, together with the estimates of plasmid size/shape is not conclusive, it is plausible to admit that only a small fraction of the internal void volume of the two resins is accessible to the long (≈3700 Å) and thin (113 Å) plasmid molecules. Therefore the majority of the binding is most certainly occurring at the outer surface of the resins. This explains the low capacity of Q-Sepharose (40 μg/ml gel) when compared with the values reported by the manufacturer for proteins (120 mg/ml gel for human serum albumin). It should be stressed at this point that the model plasmid used in this work, pUC18, is one of the smallest (2.7 kbp) currently in use in molecular biology. For gene therapy applications, plasmids containing large human genes may be expected to have as much as 15 kbp. A corollary of these observations is that the development of chromatographic matrices with very large pores (hence higher binding capacity) is desirable for the purification of plasmids at a process scale, specially if gene therapy (hence, large plasmids) applications are envisaged. In spite of the low capacity Q-Sepharose, this gel enabled the separation of supercoiled plasmid from low-molecular-mass RNA and from denatured and open circular plasmid variants. Scale-up was straightforward, and consistent results were obtained in terms of yield (62%), purity, quality and elution profiles in all three columns tested.

The presence of endotoxins (lipopolysaccharides) in the isolated supercoiled plasmid fractions was not tested in this work. However and due to the polyanionic nature of these molecules, it is likely that some residual contamination remains in the final preparation. For gene therapy applications, clearance of endotoxins constitutes an US Food and Drug Administration (FDA) requirement [3]. With the process flow diagram used here, this could be achieved with the inclusion of a final gel filtration step (for instance with Sephacryl S1000) [5].

Acknowledgements

D.M.F.P. acknowledges a grant (7/B/96/PO) from NATO/JNICT (Portugal) and T.S. a grant from the Swiss National Fonds (Switzerland). The authors would like to thank one of the referees for suggesting the hydrophobic hypothesis as an explanation for the elution order inversion when switching between Q-Sepharose and POROS columns.

Appendix A

Estimation of plasmid dimensions [6,7]

The number of times two strands of a DNA double helix in a plasmid are intertwined is called the linking number, Lk. An open circular plasmid has a linking number Lk_o which is equal to the number of base pairs in the molecule divided by the helical repeat (10.6 bp/turn). For pUC18, $Lk_o = 2686/10.6 \approx 253$. Negatively supercoiled plasmids are characterised by a deficiency in the linking number, that is, $Lk < Lk_o$. The degree of supercoiling of a plasmid can thus be expressed in terms of a specific linking number difference, or superhelix density, σ, given by:

$$\sigma = (Lk - Lk_o)/Lk_o$$

Most supercoiled plasmid molecules isolated from prokaryotes have σ values between -0.05 and -0.07 [6]. At this degree of supercoiling, plasmid molecules have a definite branched shape [7] as illustrated in Fig. 8. Boles et al. [7] found out that for 3.5 and 7.0 kbp molecules, the superhelix axis length is independent of σ and about 41% of the total DNA length. Extrapolating this result to pUC18, gives a superhelix length of $0.41 \times 8998 = 3689$ Å. For the same plasmids, the superhelix radius, r (Å) decreased hyperbolically with the superhelix density, σ, according to the relation [7]:

$$\frac{1}{r} = 0.00153 - 0.268\sigma$$

Extrapolation to pUC18, and considering the typical σ values mentioned above, gives a superhelix diameter between 99 and 134 Å.

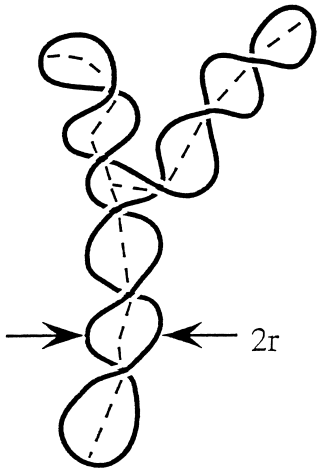

Fig. 8. Schematic model of a negatively supercoiled plasmid (adapted from Ref. [6]). The DNA double helix is represented by the thick line. The superhelix axis is the dashed curve crossing the nodes and bisecting the area enclosed by the two DNA double strands between adjacent nodes. The superhelix radius is the distance between the superhelix axis and the DNA double strands.

References

[1] F.D. Ledley, Hum. Gene Ther. 6 (1995) 1129.
[2] G.J. Nabel, E.G. Nabel, Z. Yang, B.A. Fox, G.E. Plautz, X. Gao, L. Huang, S. Shu, D. Gordon, A.E. Chang, Proc. Natl. Acad. Sci. USA 90 (1993) 11307.
[3] US FDA Hum. Gene Ther. 7 (1996) 1181.
[4] M. Marquet, N.C. Horn, J.A. Meek, BioPharm September (1996) 26.
[5] N.A. Horn, J.A. Meek, G. Budahazi, M. Marquet, Hum. Gene Ther. 6 (1995) 565.
[6] A.V. Vologodskii, S.D. Levene, K.V. Klenin, M. Frank-Kamenetskii, N.R. Cozzarelli, J. Mol. Biol. 227 (1992) 1224.
[7] T.C. Boles, J.H. White, N.R. Cozzarelli, J. Mol. Biol. 213 (1990) 213.
[8] M. Marquet, N.C. Horn, J.A. Meek, BioPharm May (1997) 42.
[9] J.K. McClung, R.A. Gonzales, Anal. Biochem. 177 (1989) 378.
[10] G. Chandra, P. Patel, T.A. Kost, J.G. Gray, Anal. Biochem. 203 (1992) 169.
[11] M. Merion, W. Warren, BioTechniques 7 (1989) 60.
[12] M. Colpan, D. Riesner, J. Chromatogr. 296 (1984) 339.
[13] R.N. Hines, K.C. O'Connor, G. Vella, W. Warren, BioTechniques 12 (1992) 430.
[14] Pharmacia Application Note, FPDA 50-01-478, Pharmacia LKB Biotechnology.
[15] J. Coffman, J. Eldering, A. Schwarz and E. Boschetti, poster presented at Recovery of Biological Products VIII, Tucson, AZ, 1996.
[16] A.P. Green, G.M. Prior, N.M. Helveston, B.E. Taittinger, X. Liu, J.A. Thompson, BioPharm May (1997) 52.
[17] P. Wils, V. Escriou, A. Warnery, F. Lacroix, D. Lagneaux, M. Ollivier, J. Crouzet, J.-F. Mayaux, D. Scherman, Gene Ther. 4 (1997) 323.
[18] J.A. Thompson, BioChromatography 1 (1986) 68.
[19] H. Yamakawa, K. Higashino, O. Ohara, Anal. Biochem. 240 (1996) 242.
[20] A. Amsterdam, Z. Er-El, S. Shaltiel, Arch. Biochem. Biophys. 171 (1975) 673.

[21] J. Porath, T. Låås, J.-C. Janson, J. Chromatogr. 103 (1975) 49.
[22] K.-C. Loh, D.I.C. Wang, J. Chromatogr. A 718 (1995) 239.
[23] J. Sambrook, E.F. Fritsch and T. Maniatis, Molecular Cloning: A Laboratory Manual, Cold Spring Harbor Laboratory Press, Cold Spring Harbor, 2nd ed., 1989.
[24] H.C. Birnboim, J. Doly, Nucleic Acids Res. 7 (1979) 1513.
[25] M.G. Rush, R.C. Warner, J. Biol. Chem. 245 (1970) 2704.
[26] J.R. Sayers, D. Evans, J.B. Thomson, Anal. Biochem. 241 (1996) 186.
[27] P.N. Hengen, Trends Biochem. Sci. 19 (1994) 139.
[28] J.D. Watson, N.H. Hopkins, J.W. Roberts, J.A. Steitz and A.M. Weiner, Molecular Biology of the Gene, Benjamin/Cummings, Menlo Park, 4th ed., 1987, p. 257.